Open Access

Recent Progress in Materials

LIDSEN Publishing Inc.

Review

Research Progress in Enhancing Proton Conductivity of Sulfonated Aromatic Polymers with ZIFs for Fuel Cell Applications

Bita Soleimani [1], Ali Haghighi Asl [1,*], Behnam Khoshandam [1], Khadijeh Hooshyari [2]

1. Faculty of Chemical, Petroleum and Gas Engineering, Semnan University, Semnan, Iran; E-Mails: bita_soleimani@semnan.ac.ir; Ahaghighi@semnan.ac.ir; Alihaghighiasl@gmail.com; bkhoshandam@semnan.ac.ir; Bkhoshandam@gmail.com
2. Department of Chemistry, Iran University of Science and Technology, Tehran, Iran; E-Mail: khadijeh_houshyari@yahoo.com

* **Correspondence:** Ali Haghighi Asl; E-Mail: Ahaghighi@semnan.ac.ir; Alihaghighiasl@gmail.com

Academic Editor: Vesna Nikolic

Recent Progress in Materials
2024, volume 6, issue 4
doi:10.21926/rpm.2404025

Received: June 22, 2024
Accepted: October 21, 2024
Published: November 04, 2024

Abstract

The escalating global temperatures and their adverse effects underscore the growing imperative for the widespread adoption of clean fuels, notably hydrogen. Proton Exchange Membrane Fuel Cells (PEMFC) emerge as a pivotal green energy technology, facilitating electricity and water generation. The optimization of PEMFC efficiency hinges on the judicious selection and fabrication of polymer membranes. Within innovative materials, Zeolitic Imidazolate Frameworks (ZIFs) represent a novel subclass within the expansive family of Metal-Organic Frameworks (MOFs). ZIFs exhibit promising potential in PEMFCs, owing to their distinctive properties such as a substantial contact surface, inherent porosity, and a sizable pore volume. This comprehensive review delves into composite membranes featuring ZIFs, shedding light on their chemical and thermal attributes. Additionally, the exploration extends to elucidating the diverse applications of ZIF compounds, accompanied by an in-depth discussion of selected chemical and thermal properties inherent to ZIF compounds. Incorporating ZIFs into various polymers yielded intriguing outcomes, demonstrating a notable enhancement in proton conductivity. The compilation of this review aims to provide

researchers with foundational insights into the realm of ZIFs, serving as a valuable resource for future investigations and advancements in the field.

Keywords
Proton exchange membrane fuel cells; composite membrane; zeolitic imidazolate frameworks; proton conductivity

1. Introduction

Fuel cells are one of the green technologies that have attracted special attention by replacing renewable energy sources compatible with the environment, such as hydrogen, instead of fossil fuels. Because fossil fuels have many negative environmental consequences, especially in terms of climate change. The widespread consumption of fossil fuels and their consequential ecological impacts, particularly to climate change, have prompted significant efforts to identify and embrace sustainable alternatives. This increased emphasis has led to a heightened interest in investigating and utilizing eco-friendly renewable energy sources, with hydrogen gaining notable attention. In hydrogen-based energy generation, fuel cells have risen as a prominent and promising technology [1]. Within the extensive range of fuel cell varieties, Proton Exchange Membrane Fuel Cells (PEMFCs) have captured substantial interest from the research community thanks to their distinctive attributes and associated benefits. These merits include rapid start-up capabilities, exceptional efficiency, significant current density, and the ability to operate at relatively low temperatures while emitting no environmentally harmful pollutants [2]. A pivotal factor influencing the performance of PEMFCs is the proton exchange membrane. As a result, the endeavor to create a suitable membrane for practical use and expedite the commercialization of PEMFCs has become a central focus for numerous researchers [3]. Recent research endeavors have brought to light a range of sulfonated aromatic polymers (SAP) that are promising alternatives to the widely used Nafion membrane in commercial applications. These polymers encompass sulfonated poly(ether ether ketone) (SPEEK) [4], polyvinyl alcohol (PVA) [5], Poly(vinylphosphonic acid) (PVPA) [6], polystyrene sulfonate (PSS) [6], and sulfonated polyether sulfone (SPES) [7-9], among others. Because of the extensive range of potential chemical compositions, which may include partially fluorinated compounds, they exhibit significant mechanical strength and exceptional chemical and thermal stability [10]. Sulfonated polymers are generally considered to exhibit heightened efficiency in the presence of water vapor. In contrast, heat-resistant polymers with a higher degree of phosphorylation tend to display a conductivity less reliant on humidity levels [10]. Figure 1 shows the schematic of some SAP and other polymers.

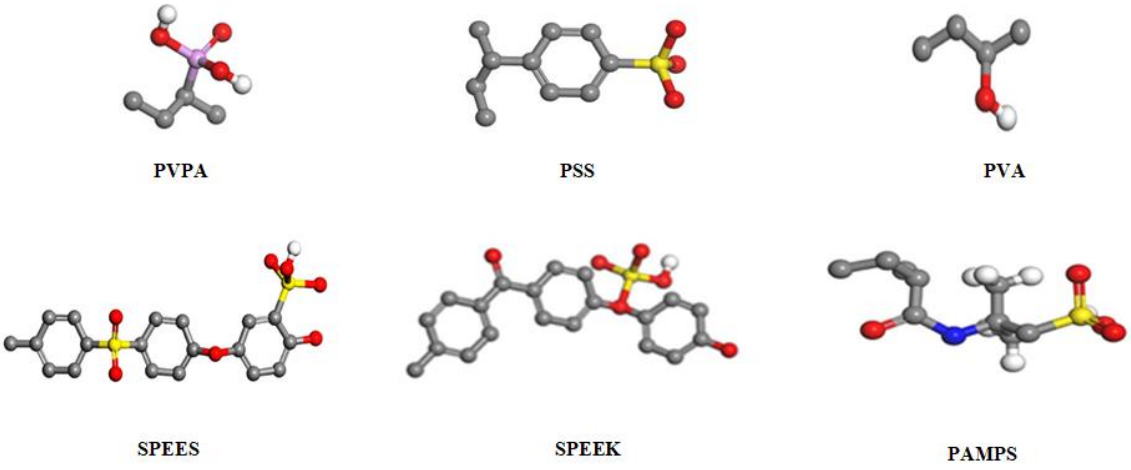

Figure 1 The structural unit of SAP polymers (S = yellow, P = purple, O = red, C = gray, N = blue, and H = white).

Moreover, a novel category of coordination polymers called metal-organic frameworks (MOFs) has garnered substantial attention. MOFs are distinguished by their composition, which involves metal clusters interconnected with organic ligands, yielding complex three-dimensional crystalline structures [11]. MOFs exhibit versatility in various applications, including storage, separation, catalysis, and even serving as carriers in medicine [12-15]. Amidst this versatility, several MOFs have shown significant promise in enabling proton and ion conduction [16-18]. The heightened proton conductivity observed in MOFs can be ascribed to their inherent design adaptability, abundant available surface area, and remarkable porosity [11, 19]. In particular, a subset of MOFs known as Zeolitic Imidazolate Frameworks (ZIFs) has demonstrated exceptional characteristics. ZIFs are constructed by linking divalent metal ions, often Zn^{2+}, with four imidazole anionic linkers. They distinguish themselves through their notably high surface area, remarkable thermal and chemical stability, and flexible, customizable structural framework [20, 21]. The presence of imidazole rings, as emphasized in the research conducted by the researchers [22-24], plays a significant role in the increased proton conductivity observed in ZIFs. Numerous research studies have introduced imidazole as an additive in membrane structures to enhance proton conductivity [24-27]. This study investigates the impact of various ZIFs when employed in different configurations to assess their influence on membrane proton conductivity. To enhance the quality of research in this field, particularly for practical applications, it is imperative to undertake a thorough review of research about (Proton Exchange Membrane) PEMs of this nature. In this context, this paper provides a comprehensive overview of research accomplishments concerning PEMs based on ZIFs, categorized by the specific polymeric matrices utilized. Research findings indicate that incorporating ZIFs into the polymer matrix enhances mechanical strength, chemical stability, and thermal resilience. Consequently, this augmentation leads to an overall improvement in the proton transfer process. Additionally, it discusses the potential directions for future development in this area.

2. ZIFs Additive in Membranes

Zeolitic Imidazolate Frameworks represent a distinct category within the realm of MOFs. ZIF materials can assume structures akin to conventional zeolites, featuring topologies such as sod, rho,

gme, lta, and ana, utilizing distinct (Imidazolate) Im ligands, as illustrated in Figure 2. The specific structure adopted by a particular ZIF is predominantly influenced by the choice of Im and solvent employed [28-32]. ZIFs are renowned for their persistent porosity and exceptional chemical and thermal stability among MOF materials. They typically feature a hydrophobic framework, even in the absence of hydrophilic functionalities in the imidazole linkers. However, the presence of hydrophilic functional groups, such as acidic and hydroxyl groups, within the ZIF structure enhances water uptake and entrapment of water molecules. Hydrophobicity and hydrophilic groups facilitate interfacial solid interactions between ZIFs and the polymer matrix in polymer–ZIF mixed matrix systems, leading to enhanced proton conductivity through the vehicle mechanism. Additionally, the imidazole rings in ZIFs significantly enhance proton transport pathways through the Grotthuss mechanism [33, 34]. This is particularly relevant when considering the imidazolate linkers utilized in constructing ZIFs.

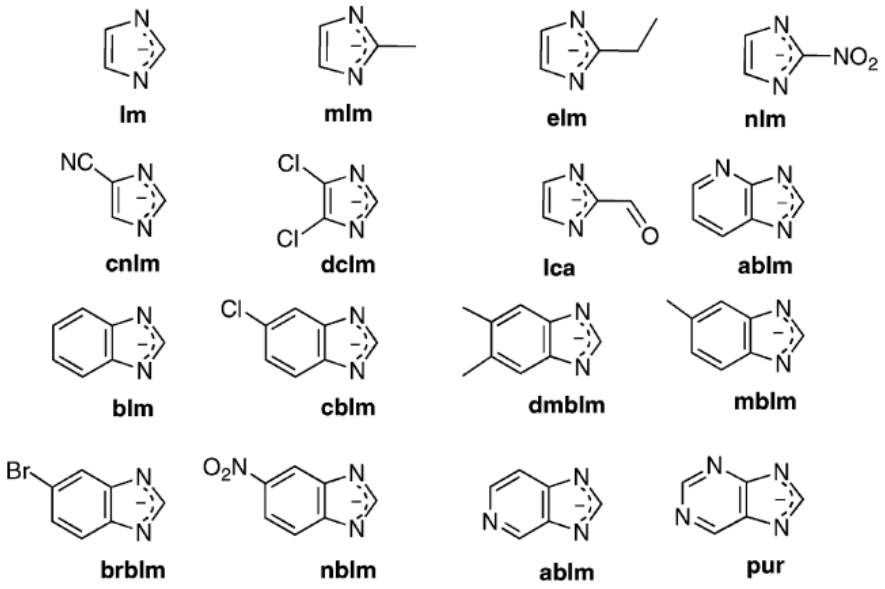

Figure 2 Exemplary instances of imidazolate linkers [31].

3. Mechanism of Proton Conductivity in Membranes

The PEMs constitute an intricate process, and this complexity is further heightened in the context of PEMs doped with MOFs. Proton conduction is a foundational aspect of PEMFC, often serving as the initial criterion in assessing membranes for potential use in fuel cells. The resistive loss is directly correlated with the ionic resistance of the membrane, underscoring the critical importance of high conductivity, particularly at elevated current densities, to ensure optimal performance. At the molecular level, the proton transport within hydrated polymeric matrices is typically elucidated through one of two principal mechanisms: (1) the "proton hopping" or "Grotthus mechanism" and (2) the "diffusion mechanism," where water serves as the vehicle, also known as the "vehicular mechanism." Understanding and optimizing these mechanisms are imperative for advancing the efficiency and overall performance of proton exchange membranes in fuel cell applications [35-37]. The simple scheme of the hopping mechanism has been shown in Figure 3 [38].

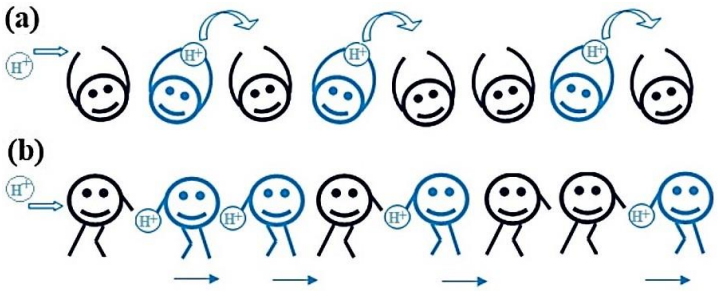

Figure 3 The simple scheme of the (a) hopping and (b) Vehicle mechanism [38].

The Grotthuss mechanism typically involves two discernible steps: initially, the proton within H_3O^+ traverses the energy barrier within the hydrogen bond, transforming H_3O^+ into H_2O. Simultaneously, the proton amalgamates with the adjacent correctly oriented H_2O, producing a new H_3O^+. Subsequently, in the second step, the initially formed H_3O^+ undergoes conversion to H_2O while acquiring new protons through rotational motion. Crucially, the orientation of the water molecule serves as the rate-controlling step for the overall proton transport. A distinctive characteristic of the Grotthuss mechanism is the sequential hopping migration of hydrated protons along the hydrogen-bonded network, a concept further refined by recent contributions from other research groups [39-42].

4. Sulfonated Aromatic Polymers (SAP)

Sulfonated aromatic polymers (SAP) have demonstrated considerable promise as materials for PEM, attributed to their elevated thermal and chemical stability, coupled with a more cost-effective production than commercially available perfluoro sulfonated polymers. The most widely recognized electrolyte membrane capable of meeting the requirements was developed by DuPont and introduced under the trademark name Nafion [10, 43-45]. The structure incorporates a perfluorosulfonic acid ionomer, as illustrated in Figure 4. Despite its efficacy, the Nafion membrane exhibits significant drawbacks, notably the utilization of highly toxic chemicals in its production, a substantial production cost exceeding $1000 per square meter, and suboptimal performance at temperatures surpassing 80°C, with proton conductivity falling below 1×10^{-3} S cm^{-1} at 100°C [44, 45].

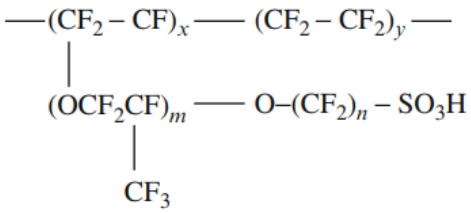

Figure 4 Perfluorosulfonic acid ionomer [46].

Many researchers have directed their efforts towards the development of proton-conductive membranes using sulfonated aromatic polymers (SAP), driven by their requisite high chemical and mechanical stability for proton-exchange membranes [24]. Among the commonly studied SAPs are SPEEK [47-49], polyether sulfone (SPES) [50, 51], polyphenyl sulfone (SPPSU) [51, 52], etc. These

SAPs are composed of relatively economical yet robust aromatic polymers. The inherent aromaticity of these macromolecular chains facilitates a neat stacking arrangement, fostering strong intramolecular π-π interactions. This property not only imparts film-forming capabilities to the polymer but also contributes to its high mechanical and chemical stability [53, 54]. Subsequently, thorough investigations have been conducted on several SAP/ZIF composite membranes.

4.1 Sulfonated Poly(Ether Ether Ketone) (SPEEK)

Polyether-ether-ketone (PEEK) is an aromatic semicrystalline polymer characterized by phenyl rings connected by ether and carbonyl (−CO−) groups. These polymers are distinguished by their exceptional thermal stability, chemical resistance, and limited solubility in organic solvents. The introduction of sulfonic acid groups into the polymer's backbone leads to a decrease in crystallinity and an increase in solubility [55, 56]. Figure 5 illustrates a schematic of sulfonated PEEK (SPEEK). Non-sulfonated PEEK polymers remain stable at temperatures up to 500°C, whereas sulfonated PEEK exhibits stability up to 240°C. Various methods for sulfonating PEEK have been explored [57, 58]. The sulfonation of PEEK proceeds via an electrophilic substitution mechanism, successfully incorporating sulfonic acid groups into the polymer structure.

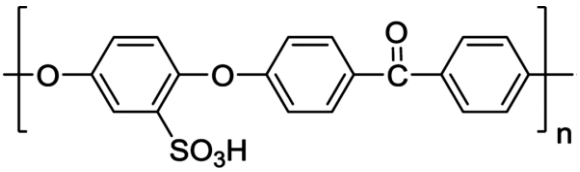

Figure 5 A schematic of SPEEK [59].

Sun et al. [60] embarked on creating PEMs by blending MOF with polymers to achieve remarkable selectivity. Their approach involved crafting two-dimensional (2D) networks by cross-linking ZIF-8 with carbon nanotubes (CNT) in a meticulously designed configuration termed ZIF-8/carbon nanotubes (ZCN). These ZCN structures were then seamlessly integrated into a series of composite PEMs by combining them with SPEEK. The electrostatic attraction between the nitrogen (N) or N-H moieties within ZIF-8 and the sulfonic acid (SO_3H) groups present in SPEEK results in a strong electrostatic interaction. Also, the π-π interactions between the 2-methylimidazole (Hmim) rings in ZIF-8 and the phenyl rings in SPEEK are responsible for the aromatic stacking forces that stabilize their interaction. Remarkably, the SPEEK/ZCN-2.5 membrane exhibited an outstanding proton conductivity of 0.05024 S cm^{-1} at 120°C and 30% RH. This achievement surpassed the proton conductivity of the pure SPEEK membrane by a factor of 11.2 (0.00450 S cm^{-1}) and that of the SPEEK/ZIF membrane by 2.1 times (0.0241 S cm^{-1}) under identical conditions (Figure 6). Additionally, the SPEEK/ZCN composite membranes substantially reduced methanol permeability.

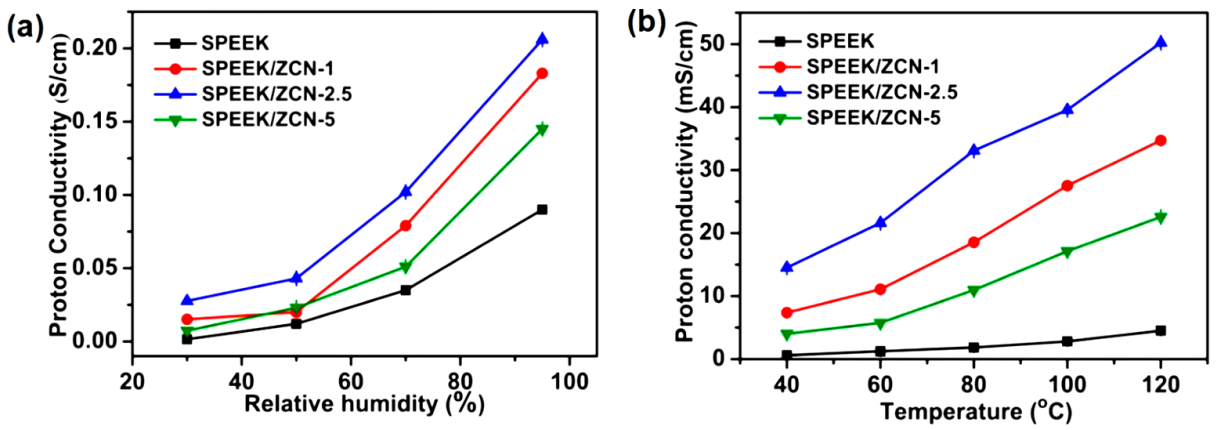

Figure 6 Evaluation of proton conductivities in SPEEK membrane and SPEEK/ZCN composite membranes under varied humidity conditions at 70°C (a) and at different temperatures at a consistent 30% RH (b) [60].

Barjola et al. [61] conducted a study where they synthesized ZIFs, including ZIF-8 (Z8), ZIF-67 (Z67), and a bimetallic Zn/Co mixture known as ZMix. These ZIFs were incorporated as additives in producing composite membranes using SPEEK as shown in Figure 7(a). This incorporation of ZIFs into the polymer matrix led to a substantial enhancement in proton transport compared to using SPEEK or ZIFs in isolation. Notably, the SPEEK/ZMix membrane exhibited the highest conductivity, particularly at elevated temperatures, outperforming both SPEEK/Z8 and SPEEK/Z67. The Bode diagrams reveal that the SPEEK/ZMix membrane's thermal activation is more pronounced than the SPEEK/Z8 and SPEEK/Z67 composite membranes (Figure 7(b)). For instance, at 120°C, the conductivity of SPEEK/ZMix reached 8.5×10^{-3} S cm^{-1}, while SPEEK/Z8 and SPEEK/Z67 showed values of 2.5×10^{-3} S cm^{-1} and 1.6×10^{-3} S cm^{-1}, respectively.

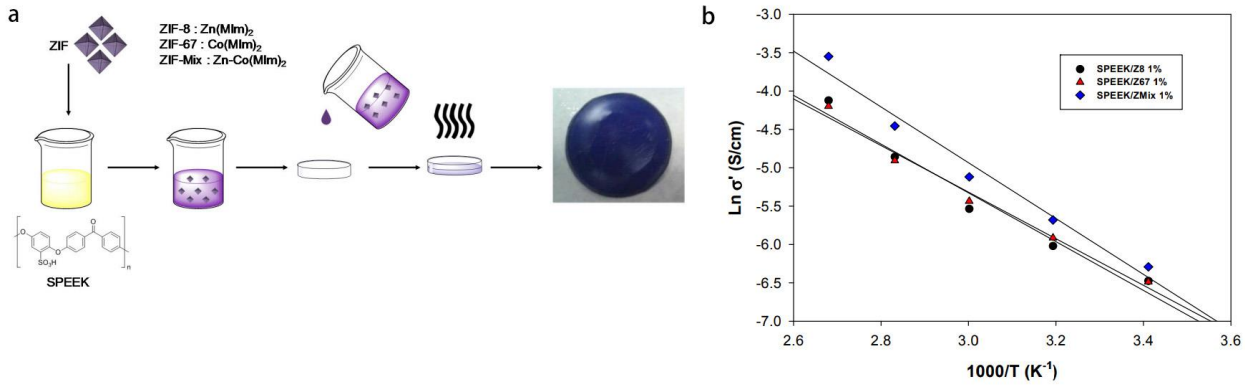

Figure 7 (a) Visualization of the membrane preparation through the casting method, (b) Arrhenius plot for SPEEK/ZIF membranes with 3 wt. % ZIF concentrations [61].

The carboxylic-functionalized Zeolitic Imidazolate Framework, designated as ZIF-COOH, was synthesized using 1H-imidazole-2-carboxylic acid as the organic linker and $Zn(NO_3)_2 \cdot 6H_2O$ as the metal center. The ZIF-COOH was then incorporated into sulfonated polyether-ether-ketone (SPEEK) to fabricate SPEEK/ZIF-COOH composite membranes. FTIR, XRD, SEM, and XPS thoroughly characterized the ZIF-COOH. The composite membranes were comprehensively analyzed, revealing significant improvements in mechanical properties, water uptake, area swelling, proton

conductivity, and methanol permeability. Specifically, Hu et al. reported that the inclusion of ZIF-COOH in SPEEK membranes led to a 42% increase in tensile strength, reaching 44.1 MPa, a 46% enhancement in proton conductivity, and a tenfold reduction in methanol permeability, down to 1.1×10^{-7} cm^2 s^{-1}. As illustrated in Figure 8, the proton conductivity of SPEEK/ZIF-COOH reached 0.0152 S cm^{-1} at 80°C, a 46.2% improvement compared to recast SPEEK [62].

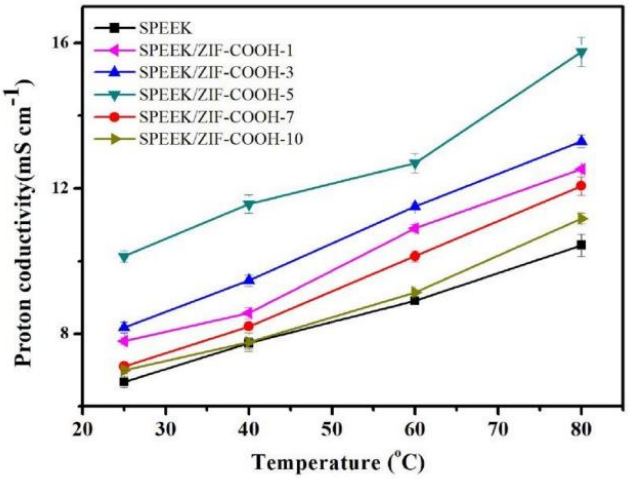

Figure 8 Proton conductivity of SPEEK/ZIF-COOH membranes [62].

In 2021, Liu's research team [63] successfully synthesized a nanocomposite, referred to as ZIF-L@GO, by merging two-dimensional Zeolitic Imidazolate Framework crystals featuring cushion-shaped cavities and leaf-like morphology (referred to as ZIF-L) and embedding them onto graphene oxide (GO) sheets via an in-situ growth approach. This composite material was then seamlessly integrated into the matrix of SPEEK, yielding a series of composite membranes named SPEEK/ZIF-L@GO. The outstanding physical, chemical, and electrochemical properties of these SPEEK/ZIF-L@GO composite membranes can be attributed to the distinctive two-dimensional superstructure of ZIF-L@GO. When the ZIF-L@GO content was controlled below 7% by weight, a harmonious compatibility between ZIF-L@GO and SPEEK was observed, with ZIF-L@GO being uniformly dispersed within the SPEEK matrix. These composite films demonstrated stability at temperatures under 290°C. Additionally, the composite membranes exhibited remarkable mechanical strength, with SPEEK/ZIF-L@GO-5 (comprising 5% ZIF-L@GO-5) boasting a tensile strength of 66.6 MPa and an elongation at break of 22.2%. Notably, in comparison to the pure SPEEK film, SPEEK/ZIF-L@GO displayed reduced water absorption and swelling tendencies. This reduction can be attributed to the lower hydrophilicity of oxygen (O) atoms and 2-methylimidazole (Hmim) units within ZIF-L@GO, in contrast to the sulfonic acid (SO_3H) groups in SPEEK. Furthermore, the diminished swelling contributed to inhibiting the diffusion of oxidative free radicals, enhancing the composite membrane's exceptional resistance to oxidative damage. Significantly, the SPEEK/ZIF-L@GO membranes exhibited higher electrical conductivity when compared to pure SPEEK, SPEEK doped with GO, and SPEEK doped with ZIF-L. The optimized SPEEK/ZIF-L@GO-5 membrane achieved an impressive electrical conductivity value (denoted as "r") of 0.183 S cm^{-1} at a temperature of 70°C and relative humidity of 90% (Figure 9). This enhanced conductivity can be ascribed to the unique two-dimensional superstructure and composition of ZIF-L@GO. For performance evaluation, a

single cell was fabricated using the SPEEK/ZIF-L@GO-5 membrane and subjected to testing under conditions of 60°C and 100% relative humidity.

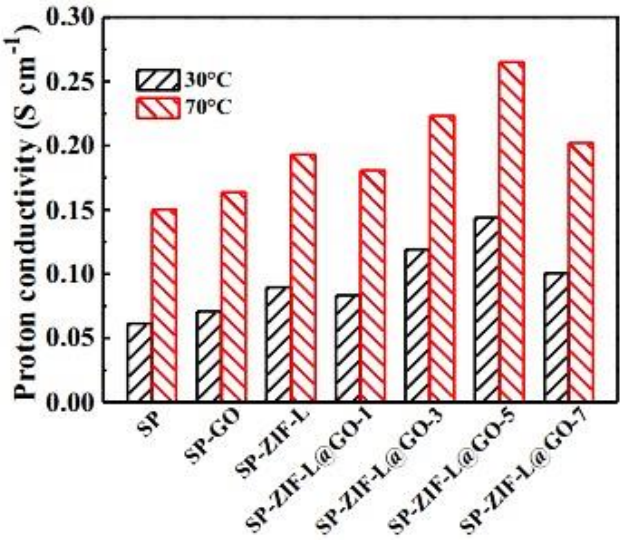

Figure 9 Proton conductivities at 30 and 70°C under 100% relative humidity [63].

In 2022, Li and their research team [64] conducted an extensive study to improve the performance of SPEEK membranes. Their approach involved the concurrent incorporation of sulfonated Zeolitic Imidazolate Framework-derived porous carbon (ZIF-C-SO_3H) and sulfonated silica ($SSiO_2$) into the membrane. By meticulously optimizing the proportions of ZIF-C-SO_3H and $SSiO_2$ within the SPEEK membrane, they successfully created an $SSiO_2$/ZIF-C-SO_3H@SPEEK composite membrane. This novel membrane demonstrated exceptional proton conductivity and a marked reduction in methanol permeability compared to the industry-standard Nafion 115 (Table 1). The outstanding performance of the $SSiO_2$/ZIF-C-SO_3H@SPEEK membrane primarily stemmed from its innovative co-filled structure. The introduction of ZIF-C-SO_3H bolstered proton conductivity while concurrently mitigating methanol permeability. The subsequent addition of $SSiO_2$ further minimized methanol permeability. Additionally, the interactions between ZIF-C-SO_3H, $SSiO_2$, and the SPEEK matrix improved mechanical and oxidation stability, rendering the membrane highly resistant to acid etching. Upon rigorous testing within direct methanol fuel cells (DMFCs), the $SSiO_2$/ZIF-C-SO_3H@SPEEK membrane exhibited an impressive maximum power density of 128.6 ± 4.6 mW cm^{-2}, nearly twice that of the benchmark Nafion 115.

Table 1 Properties of various membranes and composite membranes [64].

Membrane	Thickness (μm)	WU (%)	SR (%)	IEC (mmol L^{-1})	б (S cm^{-1})
SPEEK	98 ± 2.8	53.4 ± 1.9	16.8 ± 0.9	1.72 ± 0.03	0.1279
ZIF-C_3@SPEEK	98 ± 3.1	38.1 ± 2.2	14.8 ± 0.8	1.66 ± 0.02	0.1498
ZIF-C-SO_3H_3@SPEEK	99 ± 2.4	40.6 ± 2.8	15.2 ± 0.7	1.68 ± 0.03	0.1655
SiO_2_1/ZIF-C-SO_3H_3@SPEEK	98 ± 3.3	41.5 ± 1.8	15.3 ± 0.8	1.66 ± 0.02	0.1655
$SSiO_2$_1/ZIF-C-SO_3H_3@SPEEK	100 ± 2.6	41.5 ± 1.8	15.8 ± 0.6	1.67 ± 0.03	0.1649
Nafion 115	128 ± 1.2	25.3 ± 1.3	11.1 ± 0.5	0.92 ± 0.04	0.1397

In the study conducted by Xu et al., [65] ZIF-67 was meticulously grown uniformly on the surface of GO through chemical coordination (Figure 10(a)). This synthesized composite material was subsequently incorporated into a side-chain polymer membrane to create a series of side-chain sulfonated poly (arylene ether ketone sulfone) hybrid membranes, denoted as composite ZIF-67/GO. These hybrid membranes exhibited notable enhancements in proton conductivities and demonstrated exemplary chemical stabilities. Of particular significance, the hybrid membrane displayed optimal performance when adding ZIF-67/GO, which amounted to 1%. The proton conductivity of MSP-1% ZIF-67/GO reached 0.1331 S cm^{-1} (80°C, 100% RH), surpassing the conductivity of Nafion 117 at 0.100 S cm^{-1} (80°C, 100% RH) and the pure membrane (MSP) at 0.0809 S cm^{-1} (80°C, 100% RH) (Figure 10(b)). MSP-1% ZIF-67/GO exhibited a conductivity approximately 33.1% higher than Nafion 117 and an impressive 164.5% higher than MSP. The ZIF-67/GO filler played a crucial role in the series of hybrid membranes. GO, with its numerous hydrophilic groups and stable sheet-like structure, combined with the porous and rigid structure of ZIF-67, effectively confined the polymer chain. Additionally, the side-chain structure strategically positioned the hydrophilic cluster away from the main chain, rendering the activity of the hydrophilic cluster more flexible. This arrangement increased the "bulk water" content and provided more efficient transport channels for protons. These findings underscore the significant potential application of metal-organic frameworks as fillers in proton exchange membranes. The hybrid membranes presented in this study (MSP-X% ZIF-67/GO) exhibit promising potential for practical applications.

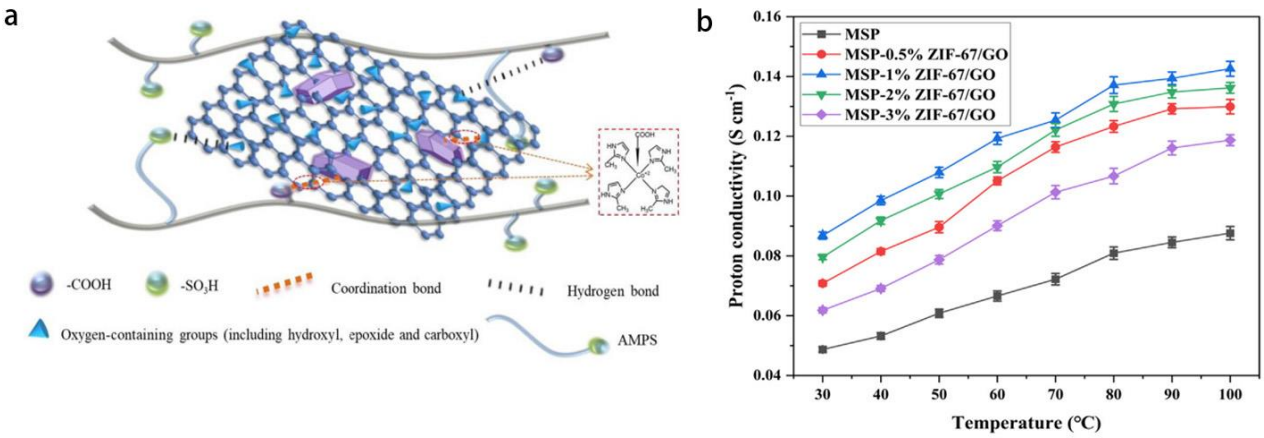

Figure 10 (a) Status of ZIF-67/GO in a polymer matrix, (b) Proton conductivities of MSP and hybrid membranes [65].

4.2 Sulfonated Poly(1,4-Phenylene Ether-Ether-Sulfone) (SPEES)

Poly(1,4-phenylene ether-ether-sulfone) (PEES) stands out as a high-performance engineering thermoplastic renowned for its exceptional film-forming properties and elevated thermal resistance [66]. Consequently, sulfonated PEES (SPEES) hold significant promise as a polymer electrolyte membrane in PEMFC (Figure 11). This potential arises from its heightened proton conductivity in comparison to similar membranes like SPEEK and sulfonated poly(phenylene oxide) (SPPO) [67, 68]. Another advantageous feature of this membrane is its straightforward and cost-effective preparation through the post-modification of commercially available PEES. In addition to these attributes, SPEES exhibits remarkable chemical stability, making it resistant to degradation under

harsh operating conditions typical in fuel cells. The membrane's mechanical strength is also noteworthy, ensuring durability and longevity during prolonged use. Furthermore, the adjustable degree of sulfonation in SPEES allows for fine-tuning its ion exchange capacity, enabling optimized proton transport and water management within the membrane. These combined properties make SPEES an excellent candidate for high-temperature fuel cell applications, where thermal stability and efficient proton conduction are critical [67, 68].

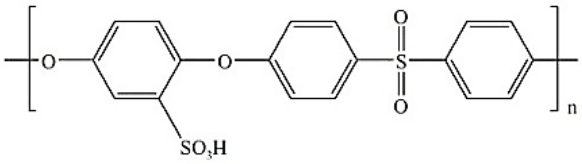

Figure 11 A schematic of the SPEES polymer [59].

While SPEES membranes demonstrate notable proton conductivity and robust thermal stability, their application in direct methanol fuel cells (DMFC) faces limitations. This restriction stems from their diminished chemical resistance to peroxide radicals and susceptibility to high methanol crossover. In the work by Soleimani et al., [69] significant attention has been devoted to PEMFCs, focusing on employing MOF/polymer nanocomposite membranes. Specifically, they introduced ZIF-90 as an additive into the SPEES matrix to explore proton conductivity in a novel nanocomposite membrane composed of SPEES/ZIF. The ZIF-90 nanostructure's unique characteristics, including high porosity, exposed surface area, and the presence of aldehyde groups, exerted a substantial influence on enhancing the mechanical, chemical, thermal, and proton conductivity properties of the SPEES/ZIF-90 nanocomposite membranes. The findings demonstrated that incorporating SPEES/ZIF-90/3 nanocomposite membranes resulted in a remarkable improvement in proton conductivity, reaching up to 160 × 10^{-3} S cm^{-1} at 90°C and 98% RH. This represented a significant advancement compared to the SPEES membrane, which exhibited a proton conductivity of 55 × 10^{-3} S cm^{-1} under identical conditions, marking a 1.9-fold increase in performance. Figure 12 presents a schematic illustrating proton conductivity at 25°C for SPEES/ZIF-90 nanocomposite membranes.

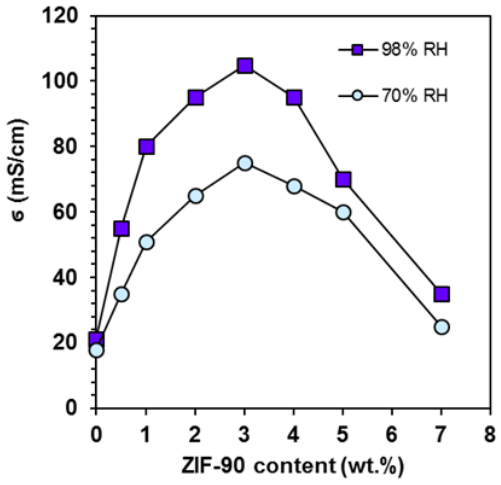

Figure 12 Proton conductivity of nanocomposite membranes at 25°C [69].

4.3 Poly(4-Styrenesulfonate) (PSS)

Poly(4-styrenesulfonate) (PSS) emerges as an auspicious material, distinguished by its water-dispersibility, favorable conductivity, cost-effectiveness, high transparency, and outstanding processability. Due to these advantageous attributes, PSS has found widespread application as host and guest materials in hybrid systems. Its utilization in such systems aims to augment electrical conductivity and overall performance, making it a versatile and extensively employed material in various applications. Furthermore, the environmental stability and scalability of PSS production make it an appealing choice for large-scale industrial applications. Its production process is cost-effective and adaptable to various manufacturing needs, ensuring that it can be produced in significant quantities without compromising on quality. This makes PSS a viable option for industries looking to reduce costs while maintaining high performance [70-72].

In 2019, Liu and colleagues devised a method to create PSS@ZIF-8 membranes. This involved loading PSS into the channels of ZIF-8 using a solid confinement conversion technique [73]. Schematic depiction of the synthesis route and structure of PSS@ZIF-8 membranes is illustrated in Figure 13.

Figure 13 Schematic depiction of the synthesis and structure of the PSS@ZIF-8 membrane [73].

The PSS threaded into ZIF-8 channels within these membranes, prevented the entanglement of PSS chains. This configuration allowed the functional sites of PSS chains within the nanochannels to come into complete contact with water, thus creating abundant pathways for proton transport without losing water as a solvent. Consequently, the PSS@ZIF-8 membrane exhibited superior proton transport capabilities compared to pure ZIF-8 crystals. Under conditions of 80°C and 100% relative humidity, the optimized PSS@ZIF-8–9 membrane achieved exceptionally high proton conductivity of 2.59×10^{-1} S cm^{-1}, with an activation energy (Ea) value of 0.543 eV, following a vehicle mechanism. Within the nanochannels of ZIF-8, the sulfonic acid groups of PSS established extensive hydrogen-bond networks with adsorbed water molecules, thereby facilitating proton hopping. Simultaneously, owing to PSS's strong hydrophilicity, a significant quantity of H_2O molecules gathered in the channels, enabling proton transport in the form of $H_5O_2^+$ and $H_9O_4^+$, which contributed to the higher Ea value of PSS@ZIF-8. Furthermore, the PSS@ZIF-8 exhibited significantly lower methanol (MeOH) permeability compared to Nafion 117, primarily due to the restricted size of the pore entrances and the fact that PSS occupied most of the nanochannel space. Thanks to its high conductivity and low permeability, the selectivity of PSS@ZIF-8–9 reached an impressive 8.17×10^6 S cm^{-1}.

4.4 Sulfonated Spiropyran

Sulfonated spiropyran polymers are smart materials known for their tunable optical and electrical properties in response to environmental stimuli such as light, pH, and temperature. Spiropyran is a small molecule with a dual structure that can switch between two structural forms: spiropyran (SP) and merocyanine (MC). This structural change, triggered by light or pH variations, alters the polymer's physical and chemical properties. Sulfonation, or the addition of sulfonic acid groups to the polymer backbone, modifies these polymers to enhance proton conductivity. As a result, sulfonated spiropyran polymers can be used in applications requiring proton conductivity, such as in PEMs. In fuel cell membranes, proton conductivity is critical for membrane efficiency. By sulfonating spiropyran polymers, the proton conductivity can be improved, thereby increasing the performance of fuel cell membranes. These membranes are essential components in fuel cells, which are used to produce clean energy. Overall, Sulfonated spiropyran polymers are attractive for advanced applications due to their ability to modulate proton conductivity in response to external stimuli. They hold promise in fields such as fuel cell membranes, sensors, and optical memory devices [74, 75].

The integration of spiropyran into MOFs, whether attached to the scaffold or embedded in the pores, has been explored. This incorporation serves diverse purposes, such as achieving photoswitching of the material's color, modulating guest molecule uptake, and exercising control over electron (hole) conductivity. In a pioneering initiative, we capitalize on the substantial change in dipole moment to profoundly influence MOF properties, emphasizing the proton-conductance of guest molecules [76].

This groundbreaking approach goes beyond merely switching alcoholic proton conduction; it extends to water, a pivotal molecule in proton conduction applications. This exploration broadens horizons by introducing spiropyran-induced modifications to tailor MOF properties, thereby presenting promising opportunities for advancements in proton-conductive materials. In 2020, Chen and their research team [77] embarked on a captivating endeavor. They employed a solid confinement conversion process to encase sulfonated spiropyran (SSP) within the confines of a ZIF-8 cavity. The outcome was the development of composite membranes denoted as SSP@ZIF-8, showcasing both high proton conductivity and responsiveness to light. SSP, a photochromic material, possesses two distinct isomeric states, MC and SP, when influenced by light. This tautomeric transformation persisted within the composite membrane, displaying a substantial isomeric transition. Notably, around 71.4% of spiropyran under thermal equilibrium transitioned into the MC form, whereas nearly 100% shifted to the SP form when exposed to visible light. The photoinduced tautomerism of SSP led to varying proton conductivity values for the SSP@ZIF-8 composite film in dark and illuminated conditions, as exemplified in Figure 14(a, b).

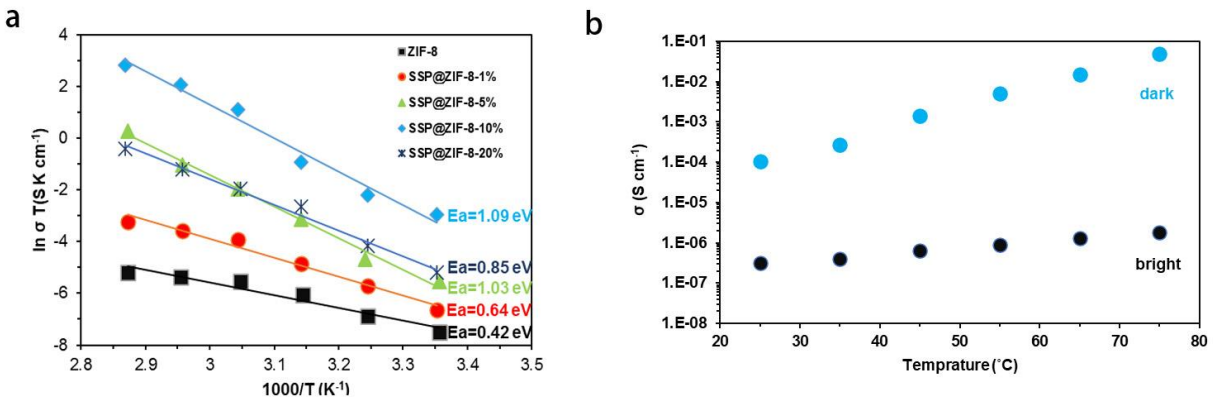

Figure 14 (a) Arrhenius diagrams of membranes with diverse SSP content at 95% RH, and (b) Proton conductivity of SSP@ZIF-8-10% membrane under visible light and in the dark [77].

In the absence of light, the composite membranes exhibited robust proton conductivity. At 25°C and 95% RH, the optimized SSP@ZIF-8–10% displayed a conductivity value (r) of 1.0×10^4 S cm^{-1}. Under conditions of 75°C and 95% RH, its conductivity reached 5.0×10^2 S cm^{-1}. However, the conductivity of the composite films experienced a significant reduction under visible light. At 25°C and 95% RH, as well as 70°C and 95% RH, the r values for SSP@ZIF-8–10% were 3.1×10^7 and 1.8×10^6 S cm^{-1}, respectively (Figure 15(a)). The substantial discrepancy in proton conductivity stemmed from the fact that, in the absence of light, SSP in its MC form contained sulfonate and phenol groups, which fostered the formation of extensive hydrogen-bonded networks with adsorbed H_2O units within the ZIF-8 cavities to facilitate proton transport. However, when subjected to visible light, SSP molecules reverted to the hydrophobic SP form, disrupting the hydrogen bond networks formed in the dark and consequently decreasing proton conductivity. Furthermore, the SSP@ZIF-8–10% composite demonstrated remarkable responsiveness to light. At 75°C and 95% RH, SSP@ZIF-8–10% achieved a swift transition from mode-to-off mode in just 5 seconds under light, exhibiting a substantial switching ratio of 2.8×10^4. Leveraging the outstanding switching characteristics of SSP@ZIF-8–10%, the researchers successfully harnessed it for remote LED lighting control by integrating it into an optical control device.

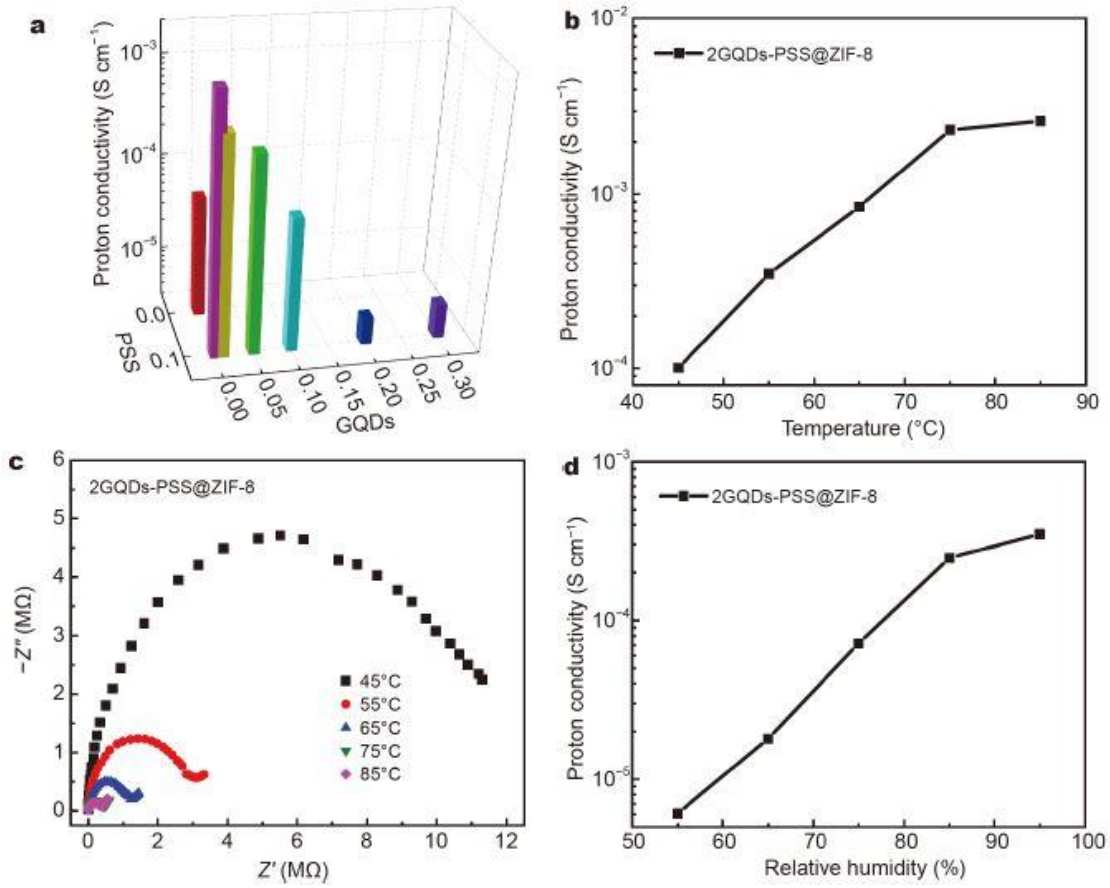

Figure 15 (a) Proton conductivities of ZIF-8, PSS@ZIF-8, and GQDs-PSS@ZIF-8 with varying GQD contents at 55°C and 95% RH. (b) Proton conductivities of 2GQDs-PSS@ZIF-8 at different temperatures and 95% RH. (c) Nyquist plots of 2GQDs-PSS@ZIF-8 corresponding to (b). (d) Proton conductivities of 2GQDs-PSS@ZIF-8 at different humilities and 55°C [78].

During that same year, Peng's research team [78] embarked on an innovative project that introduced PSS and graphene quantum dots (GQDs) into a ZIF-8 matrix through a solid-confined conversion process. This effort culminated in development of an extraordinary membrane called GQDs-PSS@ZIF-8, which exhibited photoswitchable proton-conducting capabilities. The inclusion of PSS, with its wealthy sulfonic groups, played a crucial role in enhancing the hydrophilicity of the GQDs-PSS@ZIF-8 film. In the absence of light, the proton conductivity of GQDs-PSS@ZIF-8 achieved an impressive 3.49×10^4 S cm^{-1} at 55°C and 95% RH, a value 6.3 times greater than that of the pristine ZIF-8 (Figure 15(a, b, c, d)). When exposed to light, a remarkable transformation occurred. The photoluminescence (PL) of ZIF-8 was suppressed, and the photothermal properties of GQDs caused a partial heating of the composite membrane. This rise in temperature triggered the release of water molecules from the proton transport pathway. Within minutes, the proton conductivity of the GQDs-PSS@ZIF-8 membrane dropped significantly to 2.76×10^5 S cm^{-1}, as illustrated in Figure 15. Additionally, this composite film's photoswitching proton conduction was reversible, exhibiting an impressive on/off ratio 12.8.

4.5 Other Polymers

4.5.1 Polyvinyl Alcohol (PVA)

Polyvinyl alcohol (PVA) is an exceptional biodegradable and water-soluble polymer. In contrast to the conventional polymerization process observed in most vinyl polymers, PVA is not synthesized directly from its monomer. Instead, it undergoes various indirect methods, commonly referred to as alcoholysis or hydrolysis, which involves the transformation of polyvinyl acetate [79]. PVA's unique combination of properties, including its high chemical resistance, film-forming ability, and mechanical strength, makes it versatile in various fields. In the realm of proton conductivity, PVA-based membranes have garnered significant attention, particularly in fuel cell applications. PVA is often blended with other materials, such as sulfonated polymers or inorganic fillers, which introduce additional proton-conductive pathways to enhance proton conductivity. For example, PVA can be cross-linked with sulfonated polyvinyl alcohol (SPVA) or doped with acidic groups to create a network that facilitates proton transport. These PVA-based membranes exhibit improved proton conductivity and enhanced stability and durability under fuel cell operating conditions. In summary, the ongoing research on PVA is continuously revitalized by its diverse range of applications, particularly in the development of proton-conductive membranes for clean energy technologies like fuel cells [80]. This makes PVA a promising candidate for the future of sustainable and efficient energy solutions. Ongoing research on PVA is continuously revitalized by its diverse range of applications. For example, in 2022, Panawong and their research team [81] embarked on the fabrication of proton-conducting membranes by combining double-crosslinked PVA with ZIF materials. This study sought to investigate the impact of various ZIF types, namely ZIF-8, ZIF-67, and a 1:1 weight ratio mixture (ZIF-mix), on critical membrane properties, including water uptake, ion exchange capacity (IEC), proton conductivity (б), and oxidative stability (Table 2). The composite membrane incorporating ZIF-mix exhibited the highest proton conductivity, indicating a synergistic effect arising from the combination of ZIF-8 and ZIF-67. The influence of the ZIF-mix content on the membrane properties was systematically explored, revealing an optimum loading of 7.5%. This introduction of the ZIF-mix brought about notable enhancements in proton conductivity and mechanical strength. Furthermore, all composite membranes displayed low water uptake, minimal methanol absorption, robust thermal stability (up to 140°C), and exceptional resistance to oxidative degradation. Remarkably, this work marked the first instance in which a ZIF-mix composite membrane was doped with imidazole to boost proton conductivity in non-humidified conditions. The incorporation of ZIF-mix, particularly at the 7.5% loading, significantly improved proton conductivity. Notably, a maximum proton conductivity of 7.8×10^{-3} S cm^{-1} was achieved at this loading. The proton conductivity of the imidazole-doped 7.5% ZIF-mix membrane exhibited an upward trend with increasing imidazole content and temperature. Additionally, all ZIF-mix composite membranes demonstrated low water absorption (ranging from 54.5% to 70.1%), minimal methanol uptake (45%), adequate thermal stability (up to 140°C), and high oxidative stability (70–73%). It's worth noting that under non-humidified conditions, the incorporation of imidazole resulted in a reduction in mechanical strength but was accompanied by an increase in proton conductivity. This conductivity trend continued to rise with higher imidazole concentrations and elevated temperatures. The 7.5% ZIF-mix-3Im membrane, for instance, exhibited the highest proton conductivity of 3.1×10^{-5} S cm^{-1} at 80°C (Figure 16).

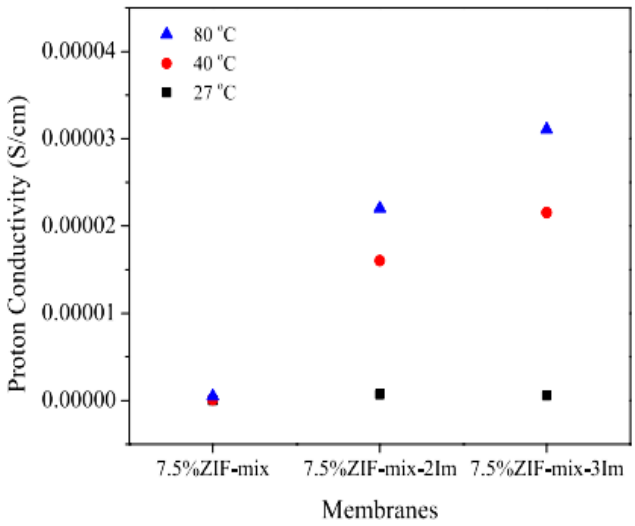

Figure 16 Proton conductivity evaluation of composite membranes doped with imidazole derived from ZIF-Mix at varied temperatures in non-humidified environments [81].

Table 2 Evaluation of water uptake, ion exchange capacity, proton conductivity, and residual weight in composite membranes with 5% loading of ZIF-8, ZIF-67, and ZIF-Mix [81].

Membrane	WU (%)	IEC (meq L^{-1})	ϭ (S cm^{-1})
5%ZIF-8	66.2 ± 4.0	2.34 ± 0.02	0.0047 ± 0.0007
5%ZIF-67	56.3 ± 0.6	2.23 ± 0.01	0.0054 ± 0.00021
5%ZIF-mix	60.0 ± 0.9	2.33 ± 0.02	0.0058 ± 0.000071

Patil et al. [82] employed a one-step polymerization technique facilitated by microwave-assisted synthesis to create copolymeric membranes. This process involved the synthesis of PVA and acrylic acid (AA) with potassium persulfate (KPS) as an initiator, forming PVA-co-AA. Simultaneously, ZIF-8 nanoparticles (NPs) were produced via the sol-gel method and seamlessly integrated in situ into the PVA-co-AA copolymers, developing the PVA-co-AAZIF-8 nanocomposite. The scanning electron microscope (SEM) image illustrates the uniform distribution of the synthesized ZIF-8 NPs within the copolymeric matrix. ZIF-8 and copolymer played distinct roles in the composite membrane as filler and adsorbent, respectively. Notably, an augmentation in the concentration of ZIF-8 filler corresponded to improved mechanical properties. The study systematically investigated fabrication parameters, such as percent composition and the quantities of copolymer and ZIF-8 incorporated into the polymer solution. The gas permeability of PVA-co-AAm/ZIF-8 nanocomposite membranes was systematically investigated by varying the ZIF-8 content as a filler at 1, 2.5, 5, and 10 wt. % concentrations. All copolymeric nanocomposite membranes underwent cross-linking with tetraethyl orthosilicate (TEOS). Fourier-transform infrared (FTIR) measurements were conducted to validate the copolymerization reaction. Surface morphology and cross-sections of the produced membranes were examined using scanning electron microscopy (SEM). The thermal stability of the membranes was assessed through thermogravimetric analysis (TGA). Subsequently, the

membranes were evaluated for their suitability in fuel cells. As the ZIF-8 content in the membranes increased, there was a proportional enhancement in ionic exchange capacity and proton conductivity. Introducing a small quantity of ZIF-8 as a filler notably improved the membrane's efficiency in terms of proton conductivity attributes. The membranes exhibited low H_2 concentration and good proton conductivity at 10^{-2} S cm^{-1} (Figure 17). The addition of a minimal quantity of ZIF-8 nanoparticles had a significant impact on the PVA-co-AA copolymeric membrane, resulting in an alteration of its properties and an increase in proton conductivity.

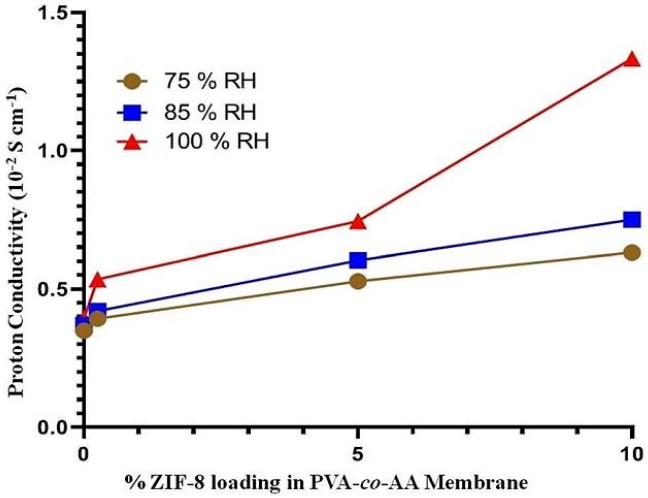

Figure 17 Proton conductivity characteristics of nanocomposites derived from PVA-co-AA copolymer infused with diverse ZIF-8 nanoparticles [82].

Erkartal et al. [83] conducted a study focused on advancing PEMs, vital components in fuel cells, actuators, and sensors. Their investigation resulted in the development of a novel composite membrane formed by combining PVA, Poly (2-acrylamido-2-methylpropane sulfonic acid) (PAMPS), and ZIF-8 using physical blending and casting techniques (refer to Figure 18).

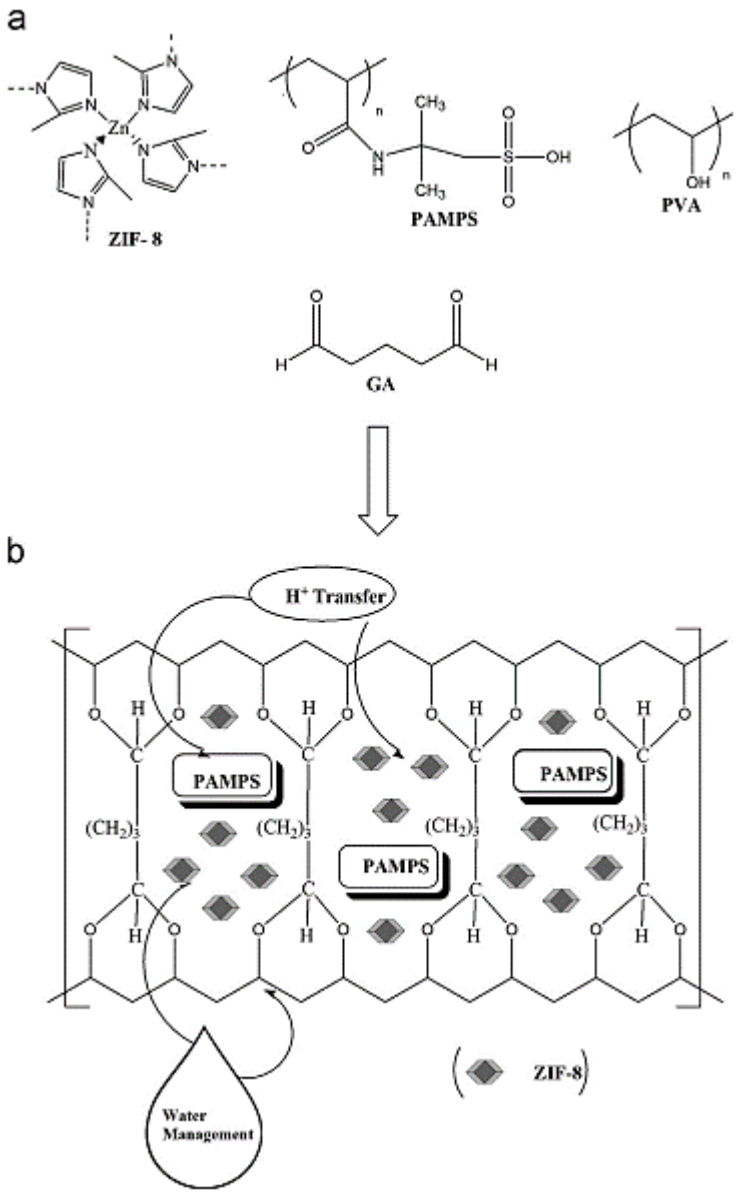

Figure 18 (a) Molecular structures of ZIF-8, PAMPS, PVA, and GA, (b) Proposed chemical configuration for the cross-linked PVA/PAMPS/ZIF-8 composite membrane [83].

They employed in situ chemical cross-linking with glutaraldehyde (GA) to enhance water management within these membranes. Various analytical methods were utilized for membrane characterization. Fourier-transform infrared spectroscopy (FT-IR) probed intermolecular and inter-polymer interactions within the membrane components while scanning electron microscopy (SEM) illuminated the membrane's structural features. X-ray diffraction (XRD) confirmed the presence of ZIF-8 nanoparticles, and thermogravimetric analysis (TGA) evaluated thermal stability. The study revealed that proton conductivity within the membranes increased with elevated temperatures and higher PAMPS content. Notably, the PVA: PAMPS: ZIF-8 (55:40:5) composition exhibited the highest proton conductivity, achieving 0.134 S cm^{-1} at 80°C under complete hydration. The study demonstrated that ZIF-8 nanoparticles bolstered proton conductivity by forming hydrogen bonds within the polymer network. Furthermore, the membrane's WU and IEC were quantified at 3.28 g g^{-1} and 1.52 meq g^{-1}, respectively (Table 3).

Table 3 Physicochemical properties of PVA/PAMPS/ZIF-8 composite membranes [83].

PVA: PAMPS: ZIF-8 Ratio (wt. %)	IEC (meq g^{-1})	WU (g g^{-1})	ϭ (S cm^{-1})
85:10:05 0.34 2.13 0.001 10.81	0.34	2.13	0.001
75:20:05 0.54 2.43 0.005 11.4	0.54	2.43	0.005
65:30:05 1.12 3.01 0.084 12.46	1.12	3.01	0.084
55:40:05 1.52 3.28 0.134 15.23	1.52	3.28	0.134
60:40:00 1.54 3.05 0.104 12.26	1.54	3.05	0.104

4.5.2 Poly(Vinylphosphonic Acid) (PVPA)

Poly(vinylphosphonic acid) (PVPA) is a promising candidate for use in proton exchange membranes (PEMs) for fuel cells, primarily due to its hygroscopic nature, which plays a significant role in its proton conductivity. The polymer's ability to absorb moisture is crucial for maintaining the water content for proton transport, a key factor in fuel cell efficiency. Comprehensive studies on PVPA have revealed that self-condensation of phosphonic acid groups within the polymer matrix poses a challenge to maximizing conductivity. This self-condensation process reduces the availability of free phosphonic acid sites, which are essential for the efficient movement of protons. While self-condensation can release some water molecules, the amount is insufficient to compensate for the reduced proton transport capacity fully. At elevated temperatures, such as 150°C under a 1-bar H_2O atmosphere, PVPA exhibits relatively modest equilibrium water content. This limitation in water retention leads to a constrained proton conductivity, measured at approximately 10^{-3} S cm^{-1}. This level may be inadequate for fuel cell applications where high proton conductivity is crucial. In conclusion, while PVPA faces inherent challenges related to self-condensation and limited water uptake, its potential for use in fuel cell applications is significant. With targeted modifications and optimization, PVPA could become an effective material for high-performance proton exchange membranes, contributing to developing more efficient and sustainable fuel cell technologies [84]. Sen et al. (2016) [85] introduced a novel method for creating functional hollow nanostructures using ZIF-8 and PVPA at room temperature. This process involves physically blending ZIF-8 and PVPA, encapsulating ZIF-8 crystallites within PVPA and the subsequent fragmentation of these crystallites (Figure 19).

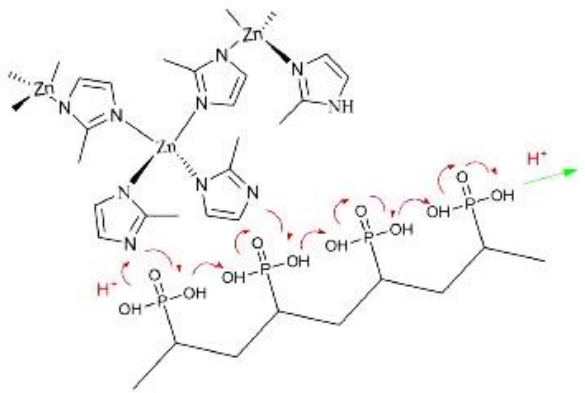

Figure 19 Proposed proton transfer mechanism in ZIF-8@PVPA hollow nanostructures, simplifying exclusion of free Hmim, free $HmimH^+$, and zinc-coordinated phosphonates [85].

The fragmentation is triggered by replacing methyl imidazolate ligands in ZIF-8 with phosphonate groups. These resulting hollow nanostructures have hybrid shells composed of PVPA, ZIF-8, and their reaction byproducts. Remarkably, these hybrid structures exhibit substantial proton conductivities that increase with temperature, even in anhydrous conditions at temperatures exceeding the boiling point of water. In Figure 20, at 140 ˚C, ZIF-8@PVPA exhibits a notable proton conductivity of 3.2 (±0.12) × 10^{-3} S cm^{-1}, surpassing the conductivity observed for PVPA or ZIF-8 in isolation. This heightened conductivity is likely ascribed to free or partially free amphoteric imidazole species within the hybrid structures. These species facilitate hydrogen-bonding interactions with phosphonate and/or phosphonic-acid units, contributing to the observed enhancement in proton conductivity.

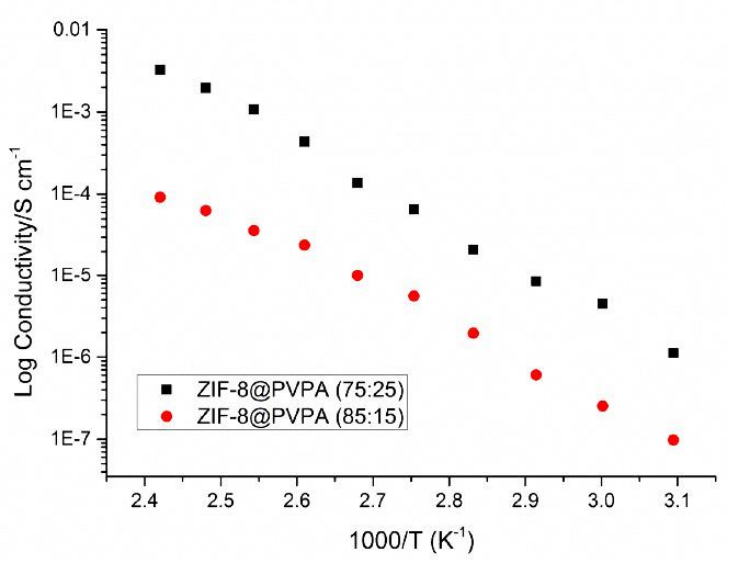

Figure 20 Arrhenius diagram for proton conductivities in ZIF-8@PVPA hollow nanostructures [85].

4.5.3 Polybenzimidazole (PBI)

Polybenzimidazole (PBI) is a high-performance polymer known for its excellent thermal stability, chemical resistance, and high mechanical strength. It is widely used in applications requiring high temperature and chemical resistance, such as in membrane technologies for fuel cells. PBI membranes, especially when doped with phosphoric acid, exhibit high proton conductivity and thermal stability, making them suitable for high-temperature PEMFCs. Several strategies can be employed to enhance proton conductivity in PBI membranes further. One approach involves optimizing the doping process to increase the concentration and distribution of phosphoric acid within the polymer matrix. Improved doping techniques can lead to a more uniform dispersion of phosphoric acid, which enhances proton conduction pathways and overall membrane performance [86]. Additionally, incorporating functional additives or fillers, such as ZIFs with different functional groups, into the PBI matrix can increase the number of proton-conducting sites and improve water retention. These additives can also enhance the membrane's mechanical properties, ensuring durability under operational conditions [87].

Escorihuela et al. report on preparing and characterizing proton-conducting composite membranes based on PBI with embedded MOF particles. Specifically, Zeolitic Imidazolate

Frameworks ZIF-8 and ZIF-67 were selected for their excellent gas separation performance. They synthesized Zn-based ZIF-8, Co-based ZIF-67, and a Zn/Co bimetallic ZIF-mix to create novel PBI composite membranes, which were doped with phosphoric acid and tested for their proton conductivity under high-temperature, anhydrous conditions. The investigation included PBI membranes with ZIF-8 and ZIF-67 additives. As illustrated in Figures 21(a) and 21(b), which show the variation in proton conductivity at different temperatures, the PBI@ZIF-8 membranes achieved a proton conductivity of 3.1×10^{-3} S cm^{-1} at 200°C. In contrast, the PBI@ZIF-67 membranes reached 4.1×10^{-1} S cm^{-1}. The incorporation of 5 wt. % of both ZIF-8 and ZIF-67 resulted in the highest conductivity of 9.2×10^{-2} S cm^{-1}, demonstrating a synergistic enhancement. These reported conductivities are among the highest achieved for mixed matrix membranes (MMMs) in high-temperature PEMFCs [87].

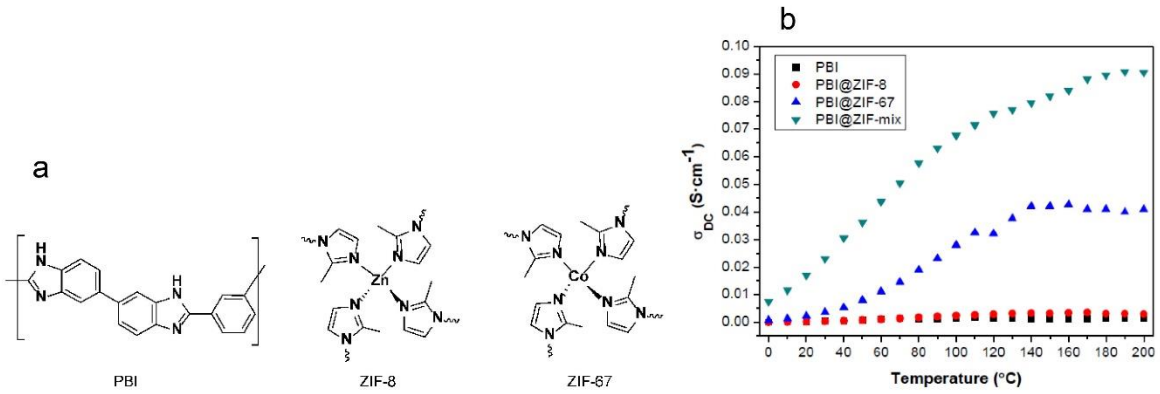

Figure 21 (a) Chemical structures of polybenzimidazole (PBI), Zeolitic Imidazolate Framework-8 (ZIF-8), and Zeolitic Imidazolate Framework-67 (ZIF-67); (b) Proton conductivity of phosphoric acid-doped PBI composite membranes with 5 wt. % ZIFs [87].

Eren et al. have developed composite membranes using PBI as the matrix and MOFs as fillers. ZIF-8 and UiO-66 MOFs were synthesized via a standard solvothermal method. The composite membranes were prepared with varying MOF loadings (2.5%, 5.0%, 7.5%, and 10.0 wt. %). Their results show a substantial enhancement in proton conductivity compared to pure PBI, with over a three-fold increase observed for PBI-UiO66 (10.0 wt. %) and PBI-ZIF8 (10.0 wt. %) membranes at 160°C. The proton conductivities of these composite membranes range from 0.225 to 0.316 S cm^{-1} at 140°C and 160°C, whereas pure PBI shows conductivities of 0.060 S cm^{-1} and 0.083 S cm^{-1} at these temperatures, respectively. However, it is also noted that the composite membranes exhibit reduced permeability and mechanical stability [88].

5. Conclusion

The burgeoning FC market stands as the primary catalyst propelling the scientific community towards the development of cost-effective and high-performance membrane materials. The production cost of proton-conducting membranes holds pivotal significance, exerting a substantial impact on the overall value of fuel cells and, consequently, the cost of energy generation. A contemporary approach aimed at enhancing membrane properties and efficiency involves the integration of Zeolitic Imidazolate Frameworks (ZIFs) into membranes. ZIFs, characterized by diverse functional groups and imidazole linkers, facilitate water retention and proton transfer, particularly

at medium to high temperatures. This article overviews research endeavors in producing polymer/ZIF composite membranes. Investigations highlight ZIF-8, ZIF-67, and ZIF-90 as prominent choices in fabricating these membranes, with ZIF-8 garnering significant attention due to its widespread commercial production and application in various polymer-based membranes. Furthermore, the inherent versatility of ZIFs allows for facile modification, incorporation of functional groups, and encapsulation of diverse additives, presenting a notable advantage. A comprehensive examination of various studies underscores that the presence of ZIFs can substantially enhance proton conductivity, thereby positively influencing the overall performance of fuel cells.

Abbreviations

abIm	5-aminobenzimidazolate
BET	Brunauer–Emmett–Teller
bIm	benzimidazolate
brbIm	5-bromobenzimidazole
cbIm	5-chlorobenzimidazolate
cnIm	4-cyanoimidazolate
CNT	carbon nanotubes
DMF	N, N-Dimethylformamide
dcIm	4,5-dichloroimidazolate
dmbIm	5,6-dimethylbenzimidazole
Ea	Energy activation
eIm	2-ethylimidazole
GQD	graphene quantum dots
GO	Graphene oxide
IEC	Ion exchange capacity
ILs	Ionic liquids
IPA	Isopropyl alcohol
Im	imidazolate
Ica	imidazolate-2-carboxyaldehyde
MOFs	Metal-organic frameworks
mbIm	5-methylbenzimidazolate
MC	merocyanine
mIm	2-methylimidazolate
nIm	2-nitroimidazolate
PVA	Polyvinyl alcohol
PVPA	Poly(vinylphosphonic acid)
PAMPS	Poly (2-acrylamido-2-methylpropane sulfonic acid)
RH	Relative humidity
SPEEK	Sulfonated poly(ether ether ketone)
SSP	sulfonated Spiropyran
SP	spiropyran
SPPO	sulfonated poly(phenylene oxide)

TGA	Thermogravimetric analysis
XPS	X-ray photoelectron spectroscopy
XRD	X-Ray Diffraction
WU	Water uptake
ZIF	Zeolitic Imidazolate Framework

Author Contributions

Conceptualization, Writing original draft – review and editing: Bita Soleimani, Supervision: Ali Haghighi Asl and Behnam Khoshandam, Formal analysis and Review: Khadije Hooshyari.

Competing Interests

The authors have declared that no competing interests exist.

References

1. Staffell I, Scamman D, Abad AV, Balcombe P, Dodds PE, Ekins P, et al. The role of hydrogen and fuel cells in the global energy system. Energy Environ Sci. 2019; 12: 463-491.
2. Karimi MB, Mohammadi F, Hooshyari K, Jalilzadeh S. Super proton conductive nafion/short fiber/nanosilica/deep eutectic solvent (DES) composite membrane for application in anhydrous fuel cells. Macromol Mater Eng. 2022; 307: 2200318.
3. Hooshyari K, Heydari S, Beydaghi H, Rajabi HR. New nanocomposite membranes based on sulfonated poly(phthalazinone ether ketone) and Fe_3O_4@SiO_2@ resorcinol–aldehyde–SO_3H for PEMFCs. Renew Energy. 2022; 186: 115-125.
4. Salarizadeh P, Javanbakht M, Askari MB, Hooshyari K, Moradi M, Beydaghi H, et al. Novel proton conducting core–shell PAMPS-PVBS@Fe_2TiO_5 nanoparticles as a reinforcement for SPEEK based membranes. Sci Rep. 2021; 11: 4926.
5. Mustafa MN, Shafie S, Wahid MH, Sulaiman Y. Light scattering effect of polyvinyl-alcohol/titanium dioxide nanofibers in the dye-sensitized solar cell. Sci Rep. 2019; 9: 14952.
6. Göktepe F, Çelik SÜ, Bozkurt A. Preparation and the proton conductivity of chitosan/poly(vinyl phosphonic acid) complex polymer electrolytes. J Non Cryst Solids. 2008; 354: 3637-3642.
7. Hooshyari K, Karimi MB, Su H, Rahmani S, Rajabi HR. Nanocomposite proton exchange membranes based on sulfonated polyethersulfone and functionalized quantum dots for fuel cell application. Int J Energy Res. 2022; 46: 9178-9193.
8. Hooshyari K, Javanbakht M, Salarizadeh P, Bageri A. Advanced nanocomposite membranes based on sulfonated polyethersulfone: Influence of nanoparticles on PEMFC performance. J Iran Chem Soc. 2019; 16: 1617-1629.
9. Mabrouk W, Ogier L, Matoussi F, Sollogoub C, Vidal S, Dachraoui M, et al. Preparation of new proton exchange membranes using sulfonated poly (ether sulfone) modified by octylamine (SPESOS). Mater Chem Phys. 2011; 128: 456-463.
10. Ivanov V, Yegorov A, Wozniak A, Zhdanovich OG, Bogdanovskaya M, Averina E. Perspective non-fluorinated and partially fluorinated polymers for low-temperature PEM FC. In: Proton exchange membrane fuel cell. London, UK: IntechOpen; 2018. pp. 35-62.

11. Furukawa H, Cordova KE, O'Keeffe M, Yaghi OM. The chemistry and applications of metal-organic frameworks. Science. 2013; 341: 1230444.
12. Omer AM, Abd El-Monaem EM, El-Subruiti GM, Abd El-Latif MM, Eltaweil AS. Fabrication of easy separable and reusable MIL-125 (Ti)/MIL-53 (Fe) binary MOF/CNT/Alginate composite microbeads for tetracycline removal from water bodies. Sci Rep. 2021; 11: 23818.
13. Zhang Q, Lei Y, Li L, Lei J, Hu M, Deng T, et al. Construction of the novel PMA@Bi-MOF catalyst for effective fatty acid esterification. Sustain Chem Pharm. 2023; 33: 101038.
14. Wang C, Liu X, Demir NK, Chen JP, Li K. Applications of water stable metal–Organic frameworks. Chem Soc Rev. 2016; 45: 5107-5134.
15. Zhang M, Zhang L, Xiao Z, Zhang Q, Wang R, Dai F, et al. Pentiptycene-based luminescent Cu (II) MOF exhibiting selective gas adsorption and unprecedentedly high-sensitivity detection of nitroaromatic compounds (NACs). Sci Rep. 2016; 6: 20672.
16. Baumann AE, Burns DA, Liu B, Thoi VS. Metal-organic framework functionalization and design strategies for advanced electrochemical energy storage devices. Commun Chem. 2019; 2: 86.
17. WU B, Pan J, Ge L, Wu L, Wang H, Xu T. Oriented MOF-polymer composite nanofiber membranes for high proton conductivity at high temperature and anhydrous condition. Sci Rep. 2014; 4: 4334.
18. Nagarkar SS, Unni SM, Sharma A, Kurungot S, Ghosh SK. Two-in-one: Inherent anhydrous and water-assisted high proton conduction in a 3D metal—Organic framework. Angew Chem Int Ed. 2014; 53: 2638-2642.
19. Sadakiyo M, Yamada T, Kitagawa H. Rational designs for highly proton-conductive metal–Organic frameworks. J Am Chem Soc. 2009; 131: 9906-9907.
20. Redfern LR, Farha OK. Mechanical properties of metal–organic frameworks. Chem Sci. 2019; 10: 10666-10679.
21. Liu C, Liu Q, Huang A. A superhydrophobic zeolitic imidazolate framework (ZIF-90) with high steam stability for efficient recovery of bioalcohols. Chem Commun. 2016; 52: 3400-3402.
22. Zhang FM, Dong LZ, Qin JS, Guan W, Liu J, Li SL, et al. Effect of imidazole arrangements on proton-conductivity in metal–organic frameworks. J Am Chem Soc. 2017; 139: 6183-6189.
23. Choi SY, Cho S, Kim D, Kim J, Song G, Singh R, et al. Boosting the proton conduction using protonated imidazole for advanced ion conducting membrane. J Membr Sci. 2021; 620: 118904.
24. Bai Z, Liu S, Chen P, Cheng G, Wu G, Liu Y. Enhanced proton conduction of imidazole localized in one-dimensional Ni-metal-organic framework nanofibers. Nanotechnology. 2020; 31: 125702.
25. Luo HB, Ren Q, Wang P, Zhang J, Wang L, Ren XM. High proton conductivity achieved by encapsulation of imidazole molecules into proton-conducting MOF-808. ACS Appl Mater Interfaces. 2019; 11: 9164-9171.
26. Zhang Z, Ren J, Xu J, Wang Z, He W, Wang S, et al. Adjust the arrangement of imidazole on the metal-organic framework to obtain hybrid proton exchange membrane with long-term stable high proton conductivity. J Membr Sci. 2020; 607: 118194.
27. Hao BB, Wang XX, Zhang CX, Wang Q. Two hydrogen-bonded organic frameworks with imidazole encapsulation: Synthesis and proton conductivity. Cryst Growth Des. 2021; 21: 3908-3915.
28. Wang B, Côté AP, Furukawa H, O'Keeffe M, Yaghi OM. Colossal cages in zeolitic imidazolate frameworks as selective carbon dioxide reservoirs. Nature. 2008; 453: 207-211.
29. Fu F, Zheng B, Xie LH, Du H, Du S, Dong Z. Size-controllable synthesis of zeolitic imidazolate framework/carbon nanotube composites. Crystals. 2018; 8: 367.

30. Huang X, Zhang J, Chen X. $[Zn(bim)_2]\cdot(H_2O)_{1.67}$: A metal-organic open-framework with sodalite topology. Chin Sci Bull. 2003; 48: 1531-1534.
31. Phan A, Doonan CJ, Uribe-Romo FJ, Knobler CB, O'keeffe M, Yaghi OM. Synthesis, structure, and carbon dioxide capture properties of zeolitic imidazolate frameworks. Acc Chem Res. 2010; 43: 58-67.
32. Banerjee R, Phan A, Wang B, Knobler C, Furukawa H, O'Keeffe M, et al. High-throughput synthesis of zeolitic imidazolate frameworks and application to CO_2 capture. Science. 2008; 319: 939-943.
33. Zhang C, Lively RP, Zhang K, Johnson JR, Karvan O, Koros WJ. Unexpected molecular sieving properties of zeolitic imidazolate framework-8. J Phys Chem Lett. 2012; 3: 2130-2134.
34. Liu XL, Li YS, Zhu GQ, Ban YJ, Xu LY, Yang WS. An organophilic pervaporation membrane derived from metal–organic framework nanoparticles for efficient recovery of bio-alcohols. Angew Chem Int Ed. 2011; 45: 10636-10639.
35. Breslau BR, Miller IF. A hydrodynamic model for electroosmosis. Ind Eng Chem Fundam. 1971; 10: 554-565.
36. De Grotthuss CJ. Memoir on the decomposition of water and of the bodies that it holds in solution by means of galvanic electricity. Biochim Biophy Acta Bioenerg. 2006; 1757: 871-875.
37. Kreuer KD, Paddison SJ, Spohr E, Schuster M. Transport in proton conductors for fuel-cell applications: Simulations, elementary reactions, and phenomenology. Chem Rev. 2004; 104: 4637-4678.
38. Pourzare K, Mansourpanah Y, Farhadi S. Advanced nanocomposite membranes for fuel cell applications: A comprehensive review. Biofuel Res J. 2016; 3: 496-513.
39. Cheng HP. The motion of protons in water–ammonia clusters. J Chem Phys. 1996; 105: 6844-6855.
40. Kulig W, Agmon N. A 'clusters-in-liquid' method for calculating infrared spectra identifies the proton-transfer mode in acidic aqueous solutions. Nat Chem. 2013; 5: 29-35.
41. Zhu A, Wang J, Han L, Fan M. Measurements and correlation of viscosities and conductivities for the mixtures of imidazolium ionic liquids with molecular solutes. Chem Eng J. 2009; 147: 27-35.
42. Pomes R, Roux B. Structure and dynamics of a proton wire: A theoretical study of H+ translocation along the single-file water chain in the gramicidin A channel. Biophys J. 1996; 71: 19-39.
43. Kraytsberg A, Ein-Eli Y. Review of advanced materials for proton exchange membrane fuel cells. Energy Fuels. 2014; 28: 7303-7330.
44. Sun X, Simonsen SC, Norby T, Chatzitakis A. Composite membranes for high temperature PEM fuel cells and electrolysers: A critical review. Membranes. 2019; 9: 83.
45. Ogungbemi E, Ijaodola O, Khatib FN, Wilberforce T, El Hassan Z, Thompson J, et al. Fuel cell membranes–Pros and cons. Energy. 2019; 172: 155-172.
46. Miyatake K. Membrane electrolytes, from perfluoro sulfonic acid (PFSA) to hydrocarbon ionomers. In: Fuel cells: Selected entries from the encyclopedia of sustainability science and technology. New York, NY: Springer; 2012. pp. 179-215.
47. Zhang W, Gogel V, Friedrich KA, Kerres J. Novel covalently cross-linked poly (etheretherketone) ionomer membranes. J Power Sources. 2006; 155: 3-12.
48. Han M, Zhang G, Li M, Wang S, Zhang Y, Li H, et al. Considerations of the morphology in the design of proton exchange membranes: Cross-linked sulfonated poly(ether ether ketone)s using

a new carboxyl-terminated benzimidazole as the cross-linker for PEMFCs. Int J Hydrog Energy. 2011; 36: 2197-2206.
49. Jun MS, Choi YW, Kim JD. Solvent casting effects of sulfonated poly (ether ether ketone) for Polymer electrolyte membrane fuel cell. J Membr Sci. 2012; 396: 32-37.
50. Tripathi BP, Chakrabarty T, Shahi VK. Highly charged and stable cross-linked 4,4'-bis(4-aminophenoxy) biphenyl-3,3'-disulfonic acid (BAPBDS)-sulfonated poly (ether sulfone) polymer electrolyte membranes impervious to methanol. J Mater Chem. 2010; 20: 8036-8044.
51. Mabrouk W, Ogier L, Vidal S, Sollogoub C, Matoussi F, Fauvarque JF. Ion exchange membranes based upon crosslinked sulfonated polyethersulfone for electrochemical applications. J Membr Sci. 2014; 452: 263-270.
52. Matsushita S, Kim JD. Organic solvent-free preparation of electrolyte membranes with high proton conductivity using aromatic hydrocarbon polymers and small cross-linker molecules. Solid State Ion. 2018; 316: 102-109.
53. Zhang Z, Wu L, Xu T. Synthesis and properties of side-chain-type sulfonated poly (phenylene oxide) for proton exchange membranes. J Membr Sci. 2011; 373: 160-166.
54. Koziara BT, Kappert EJ, Ogieglo W, Nijmeijer K, Hempenius MA, Benes NE. Thermal stability of sulfonated poly (ether ether ketone) films: On the role of protodesulfonation. Macromol Mater Eng. 2016; 301: 71-80.
55. Kerres J, Cui W, Reichle S. New sulfonated engineering polymers via the metalation route. I. Sulfonated poly (ethersulfone) PSU Udel® via metalation-sulfination-oxidation. J Polym Sci A Polym Chem. 1996; 34: 2421-2438.
56. Wnek GE, Rider JN, Serpico JM, Einset AG, Ehrenberg SG, Raboin LA. New hydrocarbon proton exchange membranes based on sulfonated styrene-ethylene/butylene-styrene triblock copolymers. ECS Proc Vol. 1995; 95-23: 247.
57. Kaliaguine S, Mikhailenko SD, Wang KP, Xing P, Robertson G, Guiver M. Properties of SPEEK based PEMs for fuel cell application. Catal Today. 2003; 82: 213-222.
58. Roziere J, Jones DJ. Non-fluorinated polymer materials for proton exchange membrane fuel cells. Annu Rev Mater Res. 2003; 33: 503-555.
59. Macksasitorn S, Changkhamchom S, Sirivat A, Siemanond K. Sulfonated poly (ether ether ketone) and sulfonated poly (1,4-phenylene ether ether sulfone) membranes for vanadium redox flow batteries. High Perform Polym. 2012; 24: 603-608.
60. Sun H, Tang B, Wu P. Two-dimensional zeolitic imidazolate framework/carbon nanotube hybrid networks modified proton exchange membranes for improving transport properties. ACS Appl Mater Interfaces. 2017; 9: 35075-35085.
61. Barjola A, Escorihuela J, Andrio A, Giménez E, Compañ V. Enhanced conductivity of composite membranes based on sulfonated poly (ether ether ketone) (SPEEK) with zeolitic imidazolate frameworks (ZIFs). Nanomaterials. 2018; 8: 1042.
62. Hu F, Wen-Chin T, Zhong F, Zhang B, Wang J, Liu H, et al. Enhanced properties of sulfonated polyether ether ketone proton exchange membrane by incorporating carboxylic-contained zeolitic imidazolate frameworks. New J Chem. 2020; 44: 13788-13795.
63. Cai YY, Zhang QG, Zhu AM, Liu QL. Two-dimensional metal-organic framework-graphene oxide hybrid nanocomposite proton exchange membranes with enhanced proton conduction. J Colloid Interface Sci. 2021; 594: 593-603.

64. Li J, Wang W, Jiang Z, Deng B, Jiang ZJ. Co-filling of ZIFs-derived porous carbon and silica in improvement of sulfonated poly (ether ether ketone) as proton exchange membranes for direct methanol fuel cells. J Power Sources. 2022; 543: 231853.
65. Xu J, Chen X, Ju M, Ren J, Zhao P, Meng L, et al. Sulfonated poly (ether ketone sulfone) composite membranes containing ZIF-67 coordinate graphene oxide showing high proton conductivity and improved physicochemical properties. J Ind Eng Chem. 2023; 119: 439-449.
66. Wang Z, Li X, Zhao C, Ni H, Na H. Sulfonated poly (ether ether sulfone) copolymers for proton exchange membrane fuel cells. J Appl Polym Sci. 2007; 104: 1443-1450.
67. Neburchilov V, Martin J, Wang H, Zhang J. A review of polymer electrolyte membranes for direct methanol fuel cells. J Power Sources. 2007; 169: 221-238.
68. Jagur-Grodzinski J. Polymeric materials for fuel cells: Concise review of recent studies. Polym Adv Technol. 2007; 18: 785-799.
69. Soleimani B, Asl AH, Khoshandam B, Hooshyari K. Enhanced performance of nanocomposite membrane developed on sulfonated poly (1,4-phenylene ether-ether-sulfone) with zeolite imidazole frameworks for fuel cell application. Sci Rep. 2023; 13: 8238.
70. Kim H, Abdala AA, Macosko CW. Graphene/polymer nanocomposites. Macromolecules. 2010; 43: 6515-6530.
71. Gaynor W, Lee JY, Peumans P. Fully solution-processed inverted polymer solar cells with laminated nanowire electrodes. ACS Nano. 2010; 4: 30-34.
72. Coates NE, Yee SK, McCulloch B, See KC, Majumdar A, Segalman RA, et al. Effect of interfacial properties on polymer-nanocrystal thermoelectric transport. Adv Mater. 2013; 25: 1629-1633.
73. Cai YY, Yang Q, Zhu ZY, Sun QH, Zhu AM, Zhang QG, et al. Achieving efficient proton conduction in a MOF-based proton exchange membrane through an encapsulation strategy. J Membr Sci. 2019; 590: 117277.
74. Mandal M, Banik D, Karak A, Manna SK, Mahapatra AK. Spiropyran–merocyanine based photochromic fluorescent probes: Design, synthesis, and applications. ACS Omega. 2022; 7: 36988-37007.
75. Rad JK, Balzade Z, Mahdavian AR. Spiropyran-based advanced photoswitchable materials: A fascinating pathway to the future stimuli-responsive devices. J Photochem Photobiol C Photochem Rev. 2022; 51: 100487.
76. Greussing V, Gallmetzer JM, Huppertz H, Hofer TS, Schwartz HA. Optical characteristics of Spiropyran@MOF composites as a function of the metal–Organic framework linker substitution. J Phys Chem C. 2022; 126: 10923-10931.
77. Liang HQ, Guo Y, Shi Y, Peng X, Liang B, Chen B. A light-responsive metal–Organic framework hybrid membrane with high on/off photoswitchable proton conductivity. Angew Chem Int Ed. 2020; 59: 7732-7737.
78. Fan S, Wang S, Wang X, Li Z, Ma X, Wan X, et al. Photogated proton conductivity of ZIF-8 membranes co-modified with graphene quantum dots and polystyrene sulfonate. Sci China Mater. 2021; 64: 1997-2007.
79. Wong CY, Wong WY, Loh KS, Daud WR, Lim KL, Khalid M, et al. Development of poly (vinyl alcohol)-based polymers as proton exchange membranes and challenges in fuel cell application: A review. Polym Rev. 2020; 60: 171-202.
80. Yoo M, Kim M, Hwang Y, Kim J. Fabrication of highly selective PVA-g-GO/SPVA membranes via cross-linking method for direct methanol fuel cells. Ionics. 2014; 20: 875-886.

81. Panawong C, Tasarin S, Phonlakan K, Sumranjit J, Saejueng P, Budsombat S. Imidazole-doped proton conducting composite membranes fabricated from double-crosslinked poly (vinyl alcohol) and zeolitic imidazolate framework. Polymer. 2022; 244: 124666.
82. Patil MB, Vader SG, Mathad SN, Patil AY, Chalawadi S, Bhajantri RF. The effect of ZIF-8 nanoparticle concentration on microwave-assisted synthesis of poly (vinyl alcohol)-co-acrylic acid copolymeric membranes and their potential application in fuel cell. Emergent Mater. 2023; 6: 755-767.
83. Erkartal M, Usta H, Citir M, Sen U. Proton conducting poly (vinyl alcohol)(PVA)/poly (2-acrylamido-2-methylpropane sulfonic acid)(PAMPS)/zeolitic imidazolate framework (ZIF) ternary composite membrane. J Membr Sci. 2016; 499: 156-163.
84. Macarie L, Ilia G. Poly (vinylphosphonic acid) and its derivatives. Prog Polym Sci. 2010; 35: 1078-1092.
85. Sen U, Erkartal M, Kung CW, Ramani V, Hupp JT, Farha OK. Proton conducting self-assembled metal–organic framework/polyelectrolyte hollow hybrid nanostructures. ACS Appl Mater Interfaces. 2016; 8: 23015-23021.
86. You Y, Deng X, Liu Q, Hou Y, Miao S. A semi-flexible polybenzimidazole with enhanced comprehensive performance for high-temperature proton exchange membrane fuel cells. Int J Hydrog Energy. 2024; 78: 879-888.
87. Escorihuela J, Sahuquillo Ó, García-Bernabé A, Giménez E, Compañ V. Phosphoric acid doped polybenzimidazole (PBI)/zeolitic imidazolate framework composite membranes with significantly enhanced proton conductivity under low humidity conditions. Nanomaterials. 2018; 8: 775.
88. Eren EO, Özkan N, Devrim Y. Preparation of polybenzimidazole/ZIF-8 and polybenzimidazole/UiO-66 composite membranes with enhanced proton conductivity. Int J Hydrog Energy. 2022; 47: 19690-19701.